

Characterization Mass Addition of Coconut Shell Carbon (rGO) to TiO₂ Using Scanning Electron Microscope (SEM) for Supercapacitor Analysis

Sinta Marito Siagian ^{*1}, Samaria Chrisna HS ^{*2}, Ferdinan Rinaldo Tampubolon ^{*2}, Suci Khairani ^{*3}, Palma Juanta ^{*4}

^{*1}Politeknik Negeri Medan, Teknik Listrik, Medan, Indonesia

^{*2}Politeknik Negeri Medan, Teknik Elektronika, Medan, Indonesia

^{*3}Politeknik Negeri Medan, Teknik Komputer, Medan, Indonesia

^{*4}Universitas Prima Indonesia, Sistem Informasi, Medan, Indonesia

Corresponding Author: sintasiagian@polmed.ac.id

ABSTRACT

This research was conducted with the aim of characterizing the semiconductor TiO₂ and coconut shell as the mass of the coconut shell increases. The study was carried out through experimental methods and characterization using SEM with three levels of magnification. The results obtained are as follows: in a 1:1 mass ratio, the particle size is 6.5 μm; in a 1:3 mass ratio, the particle size is 8.9 μm, and the largest coconut shell mass ratio is 1:5, resulting in a particle size of 7.7 μm. The differences in size in each variation are due to the physical and chemical characteristics of the observed materials, and particle size can influence the supercapacitor storage capacity.

KEYWORDS; SEM, Characterization, TiO₂, Coconut Shell, Activated Carbon

Date of Submission: 12-10-2023

Date of acceptance: 31-10-2023

I. INTRODUCTION

The use of forest biomass is not only for wood products, but also has great potential to be used as active carbon or activated charcoal with a high level of porosity. This is based on the renewable nature of biomass and the increasing demand for carbon materials as the main component in several superior strategic products ^[1]. The use of biomass waste materials as electrodes in supercapacitors, especially activated carbon (AC) derived from coconut shells, has been reported to produce superior electrode quality compared to other sources ^[2]. Coconut shell has become an attractive choice as a raw material for supercapacitor electrodes because it has a number of advantageous characteristics such as high porosity, good mechanical strength, recyclability, and low environmental impact ^[3]. Electrodes can be applied to become supercapacitors. Supercapacitors are highly efficient green energy storage devices. According to the electrochemical energy storage mechanism, supercapacitors, in terms of electrical double layer capacitors (EDLC), are considered to be the best for electricity storage. EDLC basically stores energy by absorbing electrostatic charges on the porosity of the electrode surface ^[4]. The limitation of supercapacitors lies in their inability to produce high power quickly. Supercapacitors are devices that have high specific power levels, exceeding 10 kW kg⁻¹, fast charge-discharge kinetics, good stability, and long lifetimes, often exceeding (>100,000 cycles). Because of these properties, supercapacitors are attracting great attention due to their potential to address the gap between current energy supplies requiring high currents that can be provided by conventional capacitors and the long-term energy storage provided by batteries ^[5]. Semiconductor materials that are often used as electrodes in supercapacitors are transition metal oxides such as TiO₂ (titanium dioxide) ^[6], MnO₂ (mangan dioxide) ^[7], ZnO ^[8] dan Co₃O₄ (Cobalt Oxide). Penggunaan TiO₂ (titanium dioxide) as an electrode material in supercapacitors has several advantages such as Good Electrochemical Storage Capacity, High Chemical Stability, Good Cycle Stability. In the development of supercapacitors, the electrode material selection process has a very important role. SEM can be used to study material characteristics, such as pore distribution and surface composition, which have a direct impact on supercapacitor performance ^[9]. SEM makes it possible to observe the morphology and surface structure of supercapacitor electrodes with a high level of resolution, particle size and pore

distribution. In the article created, SEM testing was carried out with 3 magnifications, namely 1000x, 2500x and 7500x. This is done so that you can see finer details on the surface of the sample, because with high resolution the identification and characterization will also be better.

II. METHODOLOGY

This research method is experimental in designing a supercapacitor prototype using a TiO₂/rGO composite material based on natural coconut shell as graphene. This design is expected to have a good function in storing energy which has variables that must be taken into account, one of which is the variable variation in mixing the TiO₂/rGO composite with the data collected later comparing the particle size and morphology of the material that has been made. The material used is TiO₂, coconut shell waste which is made into active carbon using a temperature of 400°C. Next, TiO₂ and coconut shell activated carbon are mixed using 1-Butanol. Then it is activated using sulfuric acid and then slowly adding KmnO₄ for 1 hour. Next, the samples were washed and dried, then crushed, then SEM characterization was carried out with 3 magnifications, 1000x, 2500x and 7500x.

III. RESULT VIEW

a. SEM (Scanning Electron Microscope) Analysis

SEM testing aims to observe the morphology of a surface and the shape of the particles of the prepared sample. This test uses an SEM instrument with the voltage used is 15000 kV. In synthesis, supercapacitor electrode morphology plays a role in determining the performance, efficiency, stability and safety of the device. Morphology optimization through innovative synthesis approaches and materials processing is a key research area in the development of next-generation supercapacitors. In principle, the microstructure and morphology of the material have an important role in capacitance and energy storage performance [10] Where, this analysis can study the effects on morphology which can be used to improve capacitor performance. On the surface of TiO₂:rGO it can be seen based on the following image:

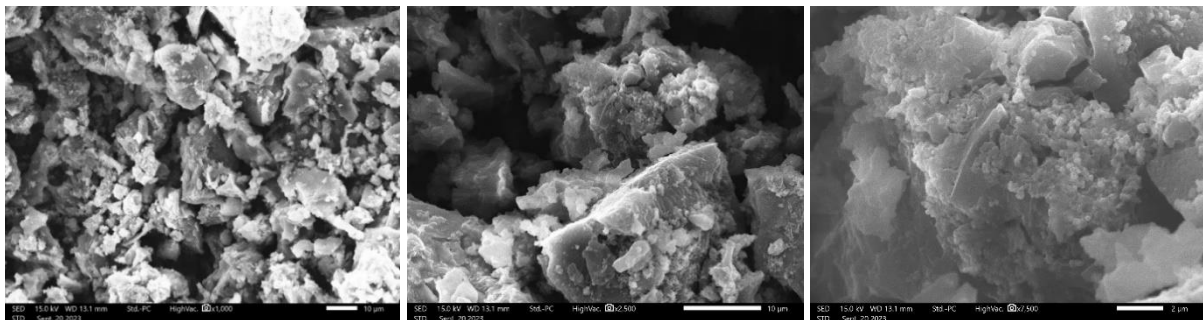


Figure 1: Morphology of mass comparison on 1:1 with magnification 1000x, 2500x dan 7500x

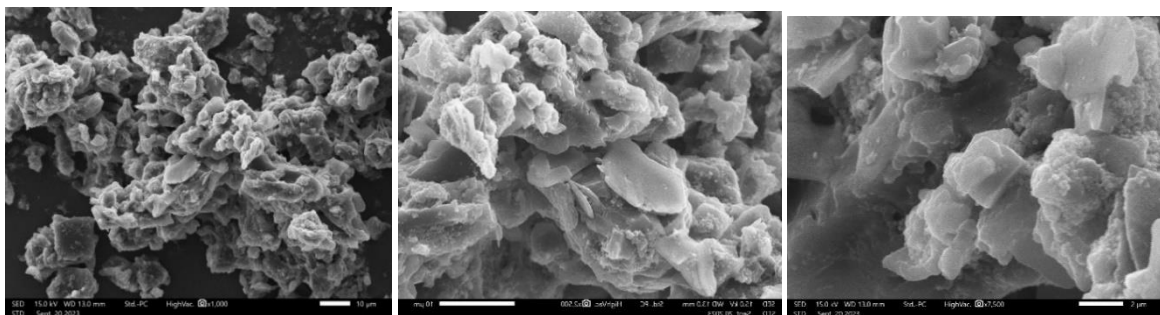


Figure 2: Morphology of mass comparison on 1:3 with magnification 1000x, 2500x dan 7500x

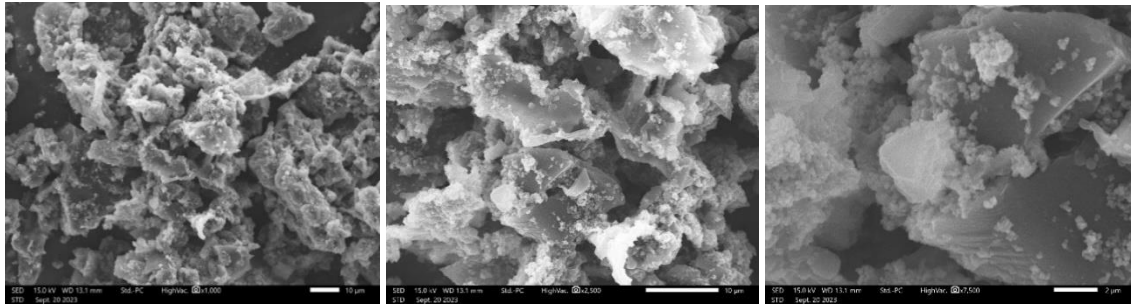


Figure 3: Morphology of mass comparison on 1:5 with magnification 1000x, 2500x dan 7500x

All composites produced with varying amounts of TiO₂ showed very similar morphological characteristics. The resulting composite shows a rod-shaped morphology, this shows similarities with the research [11]. However, in this study, the majority of morphologies tended to be round. This behavior was likely caused by changes in the monomer arrangement in local areas, which prevented the formation of elongated rod structures. Based on Figure 2 and 3, it can be seen that the distribution of particles at 1:3 and 1:5 is not evenly distributed over the entire surface and is not uniform. This could happen due to differences in chemical composition variations in consistency.

Label	Area	Mean	Min	Max	Angle	Length	
1	1236103.260	133.857	92.644	229.669	23.629	12255.267	
2	974813.140	105.796	69.444	143.372	17.496	9670.146	
3	663274.920	168.722	118.271	212.280	59.490	6516.107	
4	582877.960	170.371	114.772	215.281	-5.013	5736.066	
5	803969.600	143.006	36.943	222.822	40.914	7959.447	
6	623076.440	164.387	85.000	255.000	0.000	6115.115	
7	633126.060	128.242	88.000	187.355	-4.611	6235.542	
8	492431.380	95.028	57.979	186.000	22.249	4765.726	
9	1115507.820	191.626	152.284	244.582	26.333	11073.638	
10	452232.900	193.991	121.364	241.364	82.235	4451.724	
11	542679.480	134.582	53.000	184.127	8.746	5274.215	
12	512530.620	101.563	62.511	177.042	31.159	5037.389	
13	653225.300	121.922	83.939	202.639	122.196	6397.035	
14	552729.100	227.298	147.000	251.123	53.973	5454.070	
15	482381.760	214.521	98.000	253.000	0.000	4711.646	
16	412034.420	177.306	113.000	226.406	22.068	4002.386	
17	542679.480	204.016	164.000	240.559	24.624	5293.235	
18	623076.440	162.433	63.000	231.138	36.304	6095.363	
19	Mean	661041.671	157.704	95.620	216.875	31.211	6502.451
20	SD	229284.662	39.600	36.149	31.122	32.399	2301.262
21	Min	412034.420	95.028	36.943	143.372	-5.013	4002.386
22	Max	1236103.260	227.298	164.000	255.000	122.196	12255.267

Figure 4: Mass Compare on 1:1 Grain Measurement Results

Label	Area	Mean	Min	Max	Angle	Length	
1	457951.707	103.828	65.121	144.251	33.690	4414.042	
2	364279.767	99.771	78.612	138.851	20.556	3486.622	
3	1790174.854	74.713	39.105	157.531	132.634	17472.472	
4	1155287.261	131.519	85.835	176.759	35.417	11266.583	
5	1082431.307	102.578	62.408	206.000	71.917	10517.421	
6	291423.813	115.359	82.000	166.117	53.973	2775.232	
7	1342631.141	132.473	58.085	227.855	-18.153	13098.296	
8	697335.554	113.961	56.000	174.074	-37.569	6692.982	
9	697335.554	113.961	56.000	174.074	-37.569	6692.982	
10	801415.487	96.962	66.850	127.003	103.671	7769.579	
11	1790174.854	131.630	63.682	236.693	28.664	17440.275	
12	489175.687	88.402	55.357	139.095	23.199	4661.748	
13	Mean	913301.415	108.763	64.088	172.359	34.203	8857.353
14	SD	521404.015	17.983	13.086	35.305	51.971	5118.309
15	Min	291423.813	74.713	39.105	127.003	-37.569	2775.232
16	Max	1790174.854	132.473	85.835	236.693	132.634	17472.472

Figure 5: Mass Compare on 1:3 Grain Measurement Results

Results							
File	Edit	Font	Results				
	Label	Area	Mean	Min	Max	Angle	Length
1		799991.111	190.047	155.553	238.087	110.726	7911.972
2		559993.778	155.190	122.000	183.691	23.749	5462.570
3		799991.111	124.042	79.168	199.977	49.086	7939.729
4		679992.445	128.538	55.978	237.000	-63.435	6708.167
5		869990.333	191.879	152.562	237.473	111.801	8616.216
6		1109987.667	143.282	109.760	193.000	29.358	11014.475
7		889990.111	115.845	78.289	175.884	135.000	8768.075
8		829990.778	122.935	83.485	198.995	59.036	8163.287
9		799991.111	161.112	118.515	214.103	45.000	7919.552
10		509994.333	153.141	91.662	192.920	28.610	5011.958
11	Mean	784991.278	148.601	104.697	207.113	52.893	7751.600
12	SD	171219.202	27.033	32.890	23.249	56.956	1716.585
13	Min	509994.333	115.845	55.978	175.884	-63.435	5011.958
14	Max	1109987.667	191.879	155.553	238.087	135.000	11014.475

Figure 6. Mass Compare on 1:5 Grain Measurement Results

Based on the results of measuring the grain diameter of TiO₂ particles and coconut shell activated carbon in Figures 4, 5 and 6, the average measurement can be taken for each variation of mass comparison based on Figure 7.

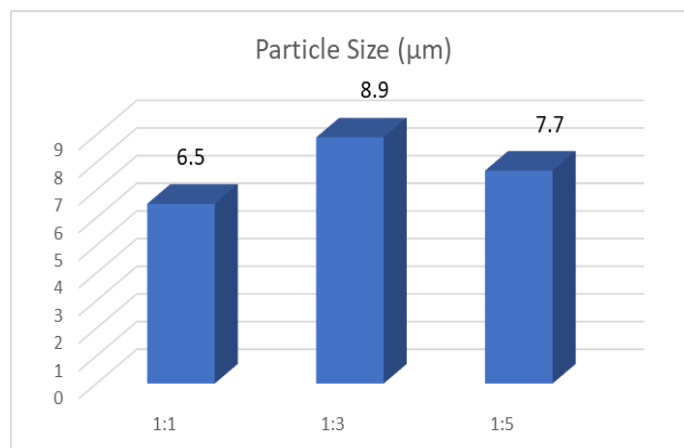


Figure 7: Diagram of Particle Size of TiO₂ : Coconut Shell

Based on Figure 8, it can be seen that the smallest particle size has a mass ratio of 1:1, while the largest particle has a mass of 1:5. Differences in particle size in the material have an influence on capacitance, this happens because when particles come into contact with electrolyte ion they can facilitate charge which of course has a role in charging and discharging supercapacitors. In this condition, the smallest particle size is 1:1, therefore efficient supercapacitor activity is at that mass ratio. The addition of carbon black to the carbon electrode changes its surface morphology. The addition of carbon black increases the number of carbon black granules covering the surface of the electrode, which likely impacts the properties of the electrode [12].

IV. CONCLUSION

From the research that has been carried out it can be concluded that all composites produced with varying amounts of TiO₂ show very similar morphological characteristics and have each particle size. At a mass ratio of 1:1, the particle size is found to be 6.5 µm, while at 1:3 the size is 8.9 µm and the largest coconut shell mass ratio is 1:5 with a particle size of 7.7 µm. The difference in size in each of these variations is due to the physical and chemical characteristics of the material being observed and the particle size can affect the storage capacity of the supercapacitor. Small particles can have a higher storage capacity because they have more active surface area. Based on research that has been carried out, the mass ratio of 1:1 has the smallest size so it has a high storage capacity compared to the others.

ACKNOWLEDGEMENTS

The author would like to thank the Medan State Polytechnic for the funding provided through Contract: B/471/PL5/PT.01.05/2023 which comes from DIPA POLMED funds in 2023.

REFERENCE

- [1] D. Alimah, "Characterization of activated charcoal microstructure porosity of cashewnut shell (*Anacardium occidentale* L.)," *Jurnal GALAM*, vol. 2, no. 1, pp. 16-28, 2021.
- [2] T. Sesuk, P. Tammawat, P. Jivaganont, K. Somton, P. Limthongkul, and W. Kobsiriphat, "Activated carbon derived from coconut coir pith as high performance supercapacitor electrode material," *Journal of Energy Storage*, vol. 25, p. 100910, 2019.
- [3] K.-C. Lee *et al.*, "Coconut shell-derived activated carbon for high-performance solid-state supercapacitors," *Energies*, vol. 14, no. 15, p. 4546, 2021.
- [4] K. Chopngam, M. Luengchavanon, M. Khangkhamano, K. Chetpattananondh, and W. Limbut, "Coating activated carbon from coconut shells with Co₃O₄/CeO₂ for high-performance supercapacitor applications: an experimental study," *BioResources*, vol. 16, no. 4, p. 8022, 2021.
- [5] C. C. Raj and R. Prasanth, "advent of TiO₂ nanotubes as supercapacitor electrode," *Journal of The Electrochemical Society*, vol. 165, no. 9, p. E345, 2018.
- [6] D. J. Ahirrao, H. M. Wilson, and N. Jha, "TiO₂-nanoflowers as flexible electrode for high performance supercapacitor," *Applied Surface Science*, vol. 491, pp. 765-778, 2019.
- [7] M. Sarif, M. Ali, Z. Zainal, M. Z. Hussein, M. H. Wahid, and N. N. Bahrudin, "Controlled concentration of Mn salt for the synthesis of manganese oxide/mesoporous carbon film as potential electrodes for supercapacitor," *Malaysian Journal of Analytical Sciences*, vol. 24, no. 2, pp. 209-217, 2020.
- [8] S. Arunpandiyan, A. Raja, S. Bharathi, and A. Arivarasan, "Fabrication of ZnO/NiO: rGO coated Ni foam binder-free electrode via hydrothermal method for supercapacitor application," *Journal of Alloys and Compounds*, vol. 883, p. 160791, 2021.
- [9] W. Trisunaryanti, *Katalis cerdas bermatriks material mesopori tercetak gelatin: sintesis dan aplikasinya*. UGM PRESS, 2022.
- [10] Y. L. Pang *et al.*, "Enhanced photocatalytic degradation of methyl orange by coconut shell-derived biochar composites under visible LED light irradiation," *Environmental Science and Pollution Research*, vol. 28, pp. 27457-27473, 2021.
- [11] M. S. H. Chowdhury *et al.*, "Easy synthesis of PPy/TiO₂/ZnO composites with superior photocatalytic performance, efficient supercapacitors and nitrite sensor," *Heliyon*, vol. 9, no. 9, 2023.
- [12] C.-H. Huang *et al.*, "Effects of TiO₂ nanoparticle doping in coconut-shell carbon on the properties of supercapacitor," *Sens. Mater.*, vol. 30, pp. 645-653, 2018.

Sinta Marito Siagian, et. al. "Characterization Mass Addition of Coconut Shell Carbon (rGO) to TiO₂ Using Scanning Electron Microscope (SEM) for Supercapacitor Analysis." *The International Journal of Engineering and Science (IJES)*, 12(10), (2023): pp. 238-242.